Kafkas Universitesi Veteriner Fakultesi Dergisi
Journal Home-Page: http://vetdergikafkas.org
E-ISSN: 1309-2251

Kafkas Univ Vet Fak Derg
32 (4): 569-583, 2026
DOI: 10.9775/kvfd.2026.36996

Research Article

Comparative Effect of Conventional and Green Silver Nanoparticles (AgNPs) on Physiological Properties, Immunity, and Oxidative Stress in N-methyl-N-nitrosourea-Induced Colon Cancer in Rat Model

Amirah S. ALAHMARI [1] (*), Sara Sabry MOHAMED [2], Alduwish Manal ABDUALLAH [3], Khalid M. ALSYAAD [4], Kamlah Ali MAJRASHI [5], Maha A. ALHASNANI [5], Amani Osman SHAKAK [5,6], Areej M. ALSOLAMI [7], Merfat O. ALJHDLI [8], Safia M.A. BAHSHWAN [5], Mada M. AL-QURASHI [5]

[1] Department of Biology, College of Science, Princess Nourah bint Abdulrahman University, P.O. Box 84428, Riyadh 11671, SAUDI ARABIA
[2] Department of Agricultural Microbiology, Faculty of Agriculture, Zagazig University, Zagazig 44511, EGYPT
[3] Department of Biology, College of Science and Humanities in Al-Kharj, Prince Sattam Bin Abdulaziz University, Alkarj 11942, SAUDI ARABIA
[4] Department of Biology, College of Science, King Khalid University, Abha, 61413, SAUDI ARABIA
[5] Biological Sciences Department, College of Science & Arts, King Abdulaziz University, Rabigh, 21911, SAUDI ARABIA
[6] Faculty of Medical Laboratory Sciences, University of Shendi, Shendi P.O. Box 142, SUDAN
[7] Department of Biology, College of Science, Jouf University, Sakaka, Al-Jouf, SAUDI ARABIA
[8] Department of Chemistry, College of Science and Arts, King Abdulaziz University, Rabigh 21911, SAUDI ARABIA

(*) **Corresponding author:**
Amirah S. Alahmari
Phone: +966 50 604460
Cellular phone: +966 50 604460
Fax: +966 50 604000
E-mail: amsalahmari@pnu.edu.sa

How to cite this article?

Alahmari AS, Mohamed SS, Abduallah AM, Alsyaad KM, Majrashi KA, Alhasnani MA, Shakak AO, Alsolami AM, Aljhdli MO, Bahshwan SMA, Al-Qurashi MM: Comparative Effect of Conventional and Green Silver Nanoparticles (AgNPs) on Physiological Properties, Immunity, and Oxidative Stress in N-methyl-N-nitrosourea-Induced Colon Cancer in Rat Model. *Kafkas Univ Vet Fak Derg*, 32 (4): 569-583, 2026.
DOI: 10.9775/kvfd.2026.36996

Article ID: KVFD-2026-36996
Received: 01.05.2026
Accepted: 19.07.2026
Published Online: 28.07.2026

Abstract

The rise of colorectal cancer and multidrug-resistant infections in immunocompromised patients demands eco-friendly therapies. This study compared conventional and green silver nanoparticles (AgNPs) synthesized via *Portulaca oleracea* leaf extract in terms of antibacterial, antioxidant, anticancer, and *in vivo* physiological activities against N-methyl-N-nitrosourea (MNU)-induced colon cancer in rats. AgNPs synthesized via *Portulaca oleracea* leaf extract exhibited an surface plasmon resonance (SPR) at 420 nm, a spherical morphology (7-22 nm), and protein capping. Against eight pathogens (including *S. aureus*, *E. coli*, and *P. aeruginosa*), green AgNPs (320 µg/mL) showed larger inhibition zones (26.3 vs. 20.1 mm for *S. aureus*) and MIC values ranging from 12.5-20 µg/mL, representing a two-fold decrease compared to chemical nanoparticles. In HCT-116 colon cancer cells, green AgNPs had a 2.3-fold lower IC_{50} (12.4 vs. 28.6 µg/mL), induced a 4.8-fold increase in Caspase-3 activity, and increased apoptotic cells to 42.6% (vs. 18.3%). In MNU-induced rat colon cancer, green AgNPs (320 mg/kg) restored physiological parameters i.e., body weight gain to 78.6% (vs. 15.4% in controls), reduced mortality to 0% (vs. 50%), lowered tumor incidence to 16.7% (vs. 100%), and normalized oxidative stress markers (MDA 2.5 vs. 8.4 nmol/mg). Preventive treatment completely abolished tumors. Green AgNPs consistently outperformed chemical counterparts, offering a potent, safe nanomedicine for dual antibacterial and anticancer applications against toxic carcinogens.

Keywords: Green silver nanoparticles, Purslane extract, Colon cancer, Antibacterial, Apoptosis, Oxidative stress, Antioxidant, Chemoprevention, Safety

Introduction

Silver nanoparticles (AgNPs) have emerged as one of the most extensively investigated nanomaterials in biomedicine due to their tunable physicochemical properties, broad-spectrum antimicrobial activity, and growing evidence of cytotoxic potential against various cancerous cells and carcinogen-induced tumor models [1]. Conventional synthesis relies predominantly on physical and chemical routes that require high energy inputs and reactive reducing agents (borohydride, hydrazine, and organic solvents). These approaches often suffer from complex purification, residual contaminants, and scalability issues, and can compromise biocompatibility and safety [2]. At the same time, the rapid expansion of AgNPs-based products for medical, pharmaceutical, and consumer applications has raised legitimate concerns about nanoparticle toxicity to cells, tissues, organs, and ecosystems, underscoring the need for safer design and rigorous toxicological assessment [3].

In response, green synthesis has gained substantial attention as an eco-friendly, cost-effective, and biocompatible alternative. Biological systems, including plants, microorganisms, and biowastes, can function as "bionanofactories," providing intrinsic reducing and capping agents that generate AgNPs under mild conditions and with lower environmental impact [4]. Plant-mediated AgNPs frequently display enhanced stability, narrow size distributions, and surface coronas rich in proteins, polysaccharides, and secondary metabolites, which can modulate their biological behavior [5].

Despite this progress, several critical gaps remain, where much of the green AgNP literature is *in vitro*, focusing on antimicrobial or cytotoxic assays, with relatively fewer systematic *in vivo* evaluations that integrate efficacy with comprehensive safety endpoints such as organ histopathology, hematology, and long-term toxicity [1]. Many green-synthesis studies emphasize plant extracts, whereas bacterial "bionanofactories" remain comparatively underexplored, even though bacteria offer fast growth, simple culture requirements, and the possibility of genetic engineering for precise control of nanoparticle properties [6]. Third, although reviews repeatedly highlight that surface chemistry, size, and shape critically influence biodistribution, toxicity, and therapeutic performance, there is still limited direct comparison between green and chemically synthesized AgNPs under identical experimental conditions, particularly in disease models such as cancer cachexia or chemoprevention [7].

Scientific evidence indicates that green AgNPs maintain a toxic profile, triggering oxidative stress, immunotoxicity, and organ injury, mediated by dose, size, functionalization, and route. Regulatory guidance for chronic or prophylactic use, especially in vulnerable populations such as cancer patients, remains fragmentary [1]. While some green-synthesized AgNPs show lower hemolysis and reduced toxicity to normal cells at therapeutic concentrations [5]. Robust *in vivo* data linking chemopreventive or anticancer efficacy to long-term safety margins remain scarce.

Within this context, the present study addresses several unmet needs. It employs a bacterial green-synthesis route, using plants as a bionanofactory and leveraging metabolites as natural reducing and capping agents. This approach is aligned with current efforts to harness microbial platforms for tunable, scalable AgNPs production, but remains less well characterized than plant-based methods [7]. The study undertakes a head-to-head comparison of green- and chemically synthesized AgNPs, examining their antimicrobial, antioxidant, and anticancer properties, as well as their *in vivo* chemopreventive efficacy in a cancer model [7]. Such parallel evaluation directly tests the common assumption, largely inferred but rarely demonstrated *in vivo*, that green AgNPs combine superior therapeutic performance with improved biosafety [8].

Beyond standard efficacy readouts, this work systematically evaluates growth performance, survival, and histological integrity of major organs, providing an integrated view of therapeutic index and subchronic toxicity that is often missing from AgNPs research. By linking restored appetite, feed efficiency, and body weight gain to tumor suppression and organ protection, the study examines whether green AgNPs can genuinely reverse cancer-associated wasting rather than merely alter weight through fluid shifts or organ hypertrophy. Finally, by defining a high-dose regimen that does not produce mortality or dose-limiting toxicity, the study contributes to the urgently needed dose-response and safety data required to guide potential chemopreventive or adjunctive use of green AgNPs in oncology [3,6]. Therefore, the main objectives of this study are to develop and characterize purslane extract-mediated green silver nanoparticles, compare them directly with conventional chemical AgNPs across multiple biological domains (antimicrobial, antioxidant, anticancer, and *in vivo* cytotoxicity activity), and rigorously assess their safety profile in terms of growth, survival, and tissue integrity.

Material and Methods

Ethical Approval

The animal study has been approved by the Unit of Biomedical Ethics, Research Ethics Committee (Ethical code number ZU-IACUC/2/F/313/2023).

Extraction and Physicochemical Properties of Purslane Extract

Aqueous extraction of dried *Portulaca oleracea* aerial parts in distilled water yielded polar bioactives. The

resulting extract was assessed for physicochemical and nutritional properties, minerals by AAS, total phenolics and flavonoids via colorimetry, and antioxidant capacity using DPPH and ABTS. Gallic acid and quercetin were further confirmed by HPLC-DAD.

Green Synthesis of Silver Nanoparticles

Silver nanoparticles were biosynthesized using aqueous purslane *(Portulaca oleracea)* leaf extract as a reducing and capping agent. The extract was heated at 45°C and filtered. Synthesis was optimized by varying $AgNO_3$:extract ratio (90:10-50:50), temperature (25-80°C), pH (3-10), and time (1-48 h). Optimal conditions (80:20, 60°C, pH 7.5, 24 h) in the dark facilitated Ag^+ reduction and capping, indicated by a reddish-brown color. Nanoparticles were harvested by centrifugation, washed with water and ethanol, then dried.

Characterization of Silver Nanoparticles

A UV-Visible spectrophotometer was used to detect surface plasmon resonance (SPR) band between 300-700 nm [9]. The morphology and shape of biosynthesized AgNPs were examined using TEM [10]. FTIR analysis was conducted to identify functional groups in the range of (4000-400 cm^{-1}) [10]. DLS and zeta potential were used to measure the size and charge of nanoparticles [10].

Antioxidant Activity

Antioxidant capacity of green and chemical AgNPs was evaluated using a freeradical scavenging assay (DPPH). Briefly, AgNPs at concentrations of 20, 40, 80, 160, and 320 µg/mL were incubated with 0.1 mM DPPH solution in methanol in the dark for a defined time, and absorbance was measured at ~517 nm. Percentage radical scavenging was calculated relative to a control without nanoparticles [11].

Antibacterial Activity

The antibacterial activity of green and chemically synthesized AgNPs was evaluated by agar well diffusion and broth microdilution methods against eight pathogenic bacterial isolates, including *Escherichia coli, Pseudomonas aeruginosa, Staphylococcus aureus, Klebsiella pneumoniae, Salmonella enterica Typhimurium, Enterococcus faecalis, Bacillus cereus*, and *Acinetobacter baumannii*. For the agar well diffusion assay, standardized inocula (0.5 McFarland) were spread on Mueller-Hinton agar plates, wells were filled with serial concentrations of AgNPs, and plates were incubated at 37°C for 18-24 h before measuring inhibition zones [10]. MICs determined by twofold serial dilution of AgNPs in Mueller-Hinton broth (96-well plates) with test bacteria; growth assessed at 660 nm [12].

In vitro Anticancer Assays

Cytotoxicity Activity: Cytotoxicity against HCT116 colon cancer cells was assessed using an MTT-type colorimetric assay [13]. Caspase-3 activation was quantified via colorimetric kit using DEVD-pNA; cleavage measured, fold change calculated. Green AgNPs gave ~4.8-fold increase vs ~2.1-fold for chemical AgNPs, indicating stronger intrinsic apoptosis, consistent with literature [14].

Expression of Bcl-2 and Bax in HCT 116 cells was evaluated post-AgNPs treatment. Proteins extracted, separated by SDS-PAGE, western-blotted, and densitometry-normalized to housekeeping for Bax/Bcl-2 ratios. Green AgNPs downregulated Bcl-2 and upregulated Bax versus chemical AgNPs, consistent with prior green AgNPs cancer studies.

Apoptosis quantified by flow cytometry (Annexin V/PI); early + late summed [14]. Green AgNPs induced ~42.6% apoptosis vs ~18.3% with the chemical.

Experimental Design for In vivo Colon Carcinogenesis: Male Albino rats (n=300; 8-10 weeks old; 180-220 g) were randomly allocated into ten experimental groups (30 rats/group) to establish an NmethylNnitrosourea (MNU)induced colon carcinogenesis model and to assess the preventive and therapeutic effects of biosynthesized (green) and chemically synthesized silver nanoparticles (AgNPs). Animals were housed under standard laboratory conditions (22±2°C, 50-60% relative humidity, 12 h light/dark cycle) with free access to standard pellet diet and water ad libitum, and were allowed one week of acclimatization before experimentation *(Fig. 1)*.

Colon carcinogenesis was induced by MNU (Sigma-Aldrich) administered either rectally or intraperitoneally at established carcinogenic doses and schedules, as previously described [15]. Following MNU exposure, rats received either green or chemical AgNPs by oral gavage at graded doses (80, 160, or 320 mg/kg body weight) once daily according to two protocols: (i) concomitant administration with MNU to evaluate chemopreventive efficacy, and (ii) delayed administration starting 4 weeks after the last MNU dose to assess therapeutic effects against established lesions. Control groups included a healthy negative control (vehicle only) and an MNUonly positive control. Throughout the experimental period, animals were monitored daily for clinical signs, and body weight and food intake were recorded weekly. At the end of the study, rats were fasted overnight, anesthetized, and euthanized; the entire colon was excised, opened longitudinally, rinsed with saline, and sampled for biochemical assays and histopathological examination.

Oxidative Stress and Antioxidant Markers in Colon Tissue

Colon segments were rapidly excised, rinsed in icecold saline, blotted, and homogenized in an appropriate buffer. The homogenates were centrifuged, and the supernatants were used to determine oxidative stress parameters. The

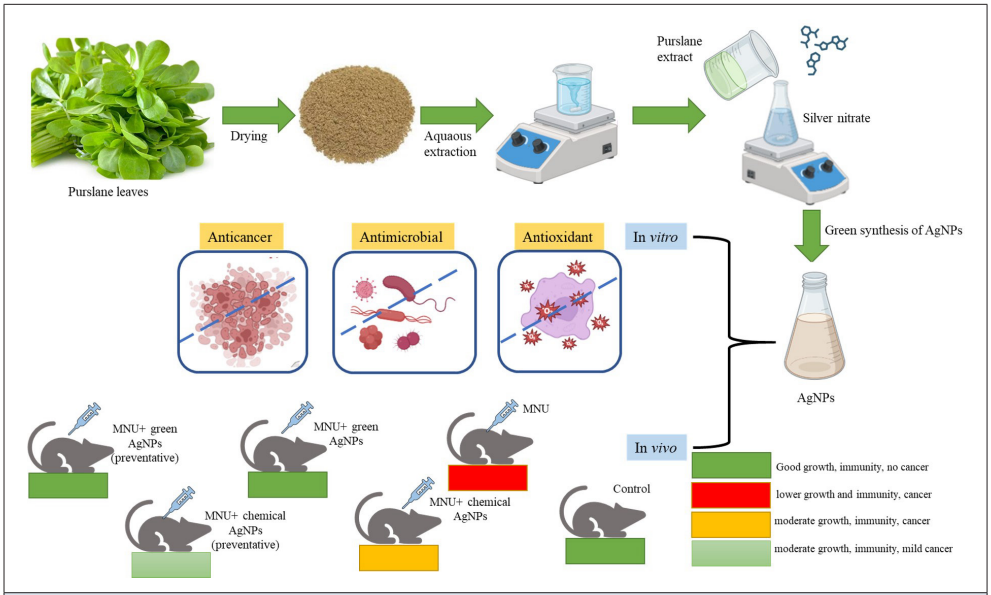

Fig 1. Experimental design of comparative effect of chemical and purslane extract silver nanoparticles with biological activities on N-methyl-N-nitrosourea rat model on growth, immunity, oxidative stress, and environmental pollution

following parameters were assessed following the methods in the study of Afrin et al.[16]. Malondialdehyde (MDA) levels were measured as an index of lipid peroxidation using the thiobarbituric acidreactive substances (TBARS) assay. Nitric oxide (NO) levels were estimated by measuring nitrite/nitrate using the Griess reaction. Antioxidant status was assessed by determining superoxide dismutase (SOD) and catalase (CAT) activities using standard spectrophotometric methods, and reduced glutathione (GSH) content using Ellman's reagent [17]. Total antioxidant capacity (TAC) was quantified using a commercial colorimetric kit following the manufacturer's instructions.

Histopathological Examination of Colon

Colon samples underwent FFPE processing (formalin fixation, graded alcohols, xylene, paraffin). Sections (4-5 µm) were cut, H&E-stained, and examined blindly by a pathologist. Crypt architecture, inflammation, dysplasia, and mucin were semi-quantitatively scored. Neoplastic lesions (adenoma, adenocarcinoma) were recorded for incidence and severity, following standard colorectal histopathology protocols [18].

Statistical Analysis

Data were expressed as mean ± standard error of the mean (SEM). All statistical analyses were executed using IBM SPSS Statistics for Windows, version 26.0 (IBM Corp., Armonk, NY, USA). Differences between groups were evaluated using one-way analysis of variance (ANOVA), followed by an appropriate post hoc multiple-comparison test (Tukey's test). A -values less than 0.05, 0.001, and 0.0001 were considered statistically significant.

Results

Physicochemical Properties of Purslane Extract

The aqueous extract of *Portulaca oleracea* L. demonstrates extraordinary nutritional density, with exceptionally high potassium (2652.00 mg/100g DW) and calcium (1005.20 mg/100g DW) *(Table 1)*, positioning it as a valuable functional food for electrolyte balance and skeletal integrity. HPLC profiling identifies gallic acid, quercetin, and ferulic acid as the dominant phenolic bioactives. Notably, total flavonoid content (133.23 mg RE/g) substantially surpasses total phenolic content (51.01 mg GAE/g), indicating that flavonoids are the principal drivers of the extract's biological efficacy. This compositional superiority translates into potent radical-scavenging capacity, with DPPH and ABTS IC_{50} values both below 60 µg/mL. Furthermore, the presence of photosynthetic pigments, including β-carotene and chlorophyll, adds synergistic photoprotective and anti-inflammatory value, broadening its therapeutic appeal.

Characterization of Silver Nanoparticles Synthesized by Purslane Extract

Biosynthesis was initially validated by UV-Vis spectroscopy, which revealed a characteristic surface plasmon resonance band centered at approximately 420 nm *(Fig. 2-A)*, confirming the successful reduction of Ag^{+} ions to metallic Ag^{0}. Transmission electron microscopy illustrated predominantly spherical nanoparticles *(Fig. 2-B)*, with a relatively narrow size distribution ranging from 7 to 22 nm *(Fig. 2-C)*. Zeta potential analysis yielded a strongly negative surface charge of -27.33 mV *(Fig. 2-D)*, ensuring

Table 1. *Chemical Composition, Antioxidant Activity, and IC50 Values of Purslane (Portulaca oleracea L.) Extracts*		
Component/Parameter	**Specific Compound/Measure**	**Specific Value (±SD)**
Macronutrients	Sodium (Na)	228.20±33.06 mg/100 g DW
	Potassium (K)	2652.00±432.1 mg/100 g DW
	Calcium (Ca)	1005.20±366.52 mg/100 g DW
	Potassium (K)	494 mg/100 g
	Magnesium (Mg)	68 mg/100 g
Phenolic Acids	Gallic acid	77.89 ppm/62.59 ppm
	Coumaric acid	19.25 ppm/16.25 ppm
	Ferulic acid	40.25 ppm/29.58 ppm
	Caffeic acid (suspected)	41.25 ppm
Flavonoids	Quercetin	58.78 ppm
	Kaempferol (Kemopferol)	24.15 ppm
Vitamins	Vitamin C	85.6 ppm
	Vitamin E	54.1 ppm
Pigments	Chlorophyll a	40.46 mg g^{-1} DW
	Chlorophyll b	9.94 mg g^{-1} DW
	β-Carotene	14.16 mg g^{-1} DW
Antioxidant Activity & IC50 Values		
Total Phenolic Content (TPC)	mg Gallic Acid Equivalent (GAE) g^{-1} DW	51.01 mg GAE g^{-1} DW
Total Flavonoid Content (TFC)	mg Rutin Equivalent (RE) g^{-1} DW	133.23 mg RE g^{-1} DW
DPPH Radical Scavenging Activity (IC_{50})	High Potency (Acetone)	57.23 µg mL^{-1}
ABTS Radical Scavenging Activity (IC_{50})	High Potency (Fresh)	52.86 µg mL^{-1}
FRAP (Ferric Reducing Antioxidant Power)	µmol Trolox Equivalent (TE) g^{-1} DW	43.5 ± 1.0 mg GAE g^{-1} DW
Ferrous Iron (Fe^{2+}) Chelating Activity	% Inhibition (Methanol extract)	12.78%
All values are presented as measurements (± standard deviation where available) on a Dry Weight (DW) basis		

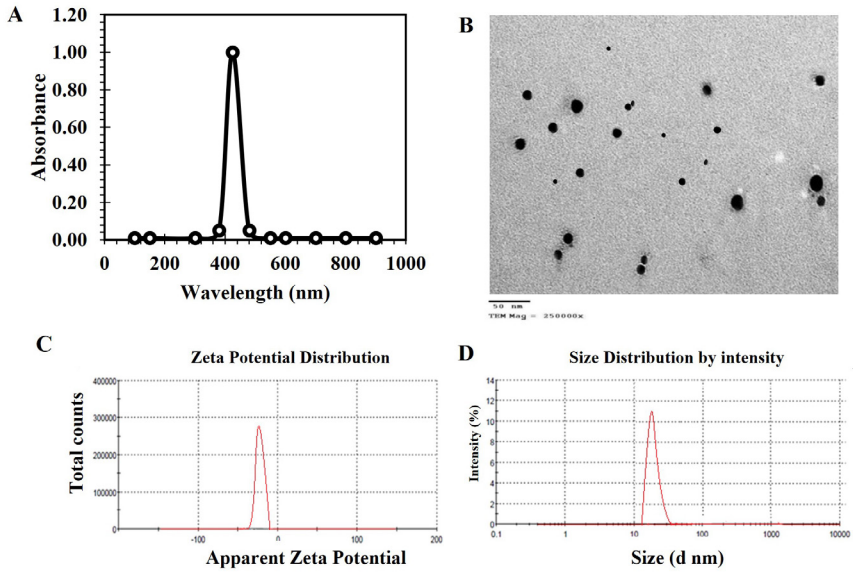

Fig 2. Characterization of green silver nanoparticles using purslane extract. **(A)** UV absorbance spectrum with peak near 420 nm indicating SPR. **(B)** TEM micrograph showing spherical AgNPs, well-dispersed, approximately 7-22 nm in size, at 250.000x magnification. **(C)** The zeta potential measures the net surface charge of AgNPs was -27.33 mV, and **(D)** the exact size of 20 nm detected by DLS zeta sizer

robust electrostatic repulsion that prevents aggregation and guarantees long-term colloidal stability in biological fluids. Dynamic light scattering corroborated these findings, placing the hydrodynamic diameter at approximately 20 nm, thus indicating a monodisperse population highly suitable for efficient cellular uptake and systemic administration.

Biological Activities

Antioxidant Activity: Both green and chemically synthesized AgNPs exhibited a clear, concentration-dependent radical-scavenging behavior. However, at every matched concentration across the tested range, green AgNPs consistently demonstrated substantially higher percentage inhibition, reaching 80-85% activity compared to the consistently lower values obtained for chemical AgNPs. This enhanced performance is synergistically augmented by the biomolecular corona comprising polyphenols, flavonoids, and organic acids that coats the green nanoparticles, providing an additional electron reservoir for efficient radical stabilization and sustained antioxidant activity *(Fig. 3)*.

Antibacterial Activity: The antimicrobial superiority of green AgNPs was systematically validated against eight clinically relevant, cancer-associated bacterial species using zone of inhibition (ZOI) and minimum inhibitory concentration (MIC) assays across 20-320 µg/mL *(Table 2)*.

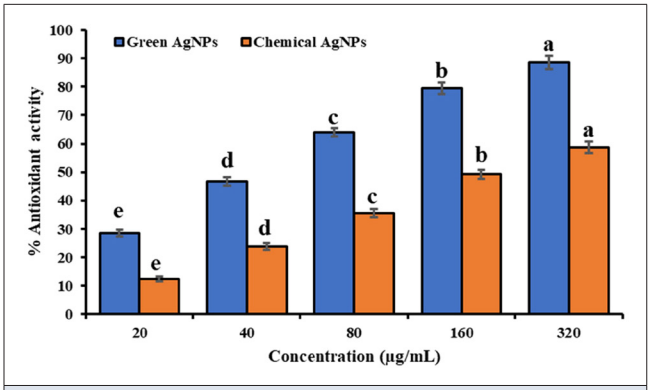

Fig 3. Antioxidant activity of green vs. chemical AgNPs against DPPH free radicals (% inhibition, mean ± SE). Values expressed as mean ± SE (n = 3). Data analyzed by two-way ANOVA (factors: nanoparticle type, concentration) followed by Tukey's post hoc test; P<0.05 considered significant. Different lowercase superscript letters within a row indicate significant differences between green and chemical AgNPs at the same concentration (P<0.05). Different uppercase superscript letters within a column indicate significant differences among concentrations for the same nanoparticle type (P<0.05)

A steep, dose-dependent increase in potency was observed; against MRSA, green AgNPs expanded the ZOI from 10.1 mm at 20 µg/mL to 26.3 mm at 320 µg/mL, whereas chemical AgNPs peaked at only 20.1 mm. The MIC data provided even stronger evidence: green AgNPs achieved an average two-fold reduction (range 1.8- to 2.5-fold) compared to chemical AgNPs, meaning equivalent bactericidal effects require substantially lower concentrations. *S. aureus* MRSA

Table 2. *Antimicrobial activity of green vs. chemical silver nanoparticles against pathogenic bacteria – Zone of Inhibition (mm ± SE) at 20-320 µg/mL and MIC (µg/mL ± SE)*

Bacterial Species	AgNPs Type	20 µg/mL	40 µg/mL	80 µg/mL	160 µg/mL	320 µg/mL	MIC (µg/mL)
Escherichia coli	Green	8.2±0.3	11.4±0.4	15.2±0.5	18.5±0.4	22.1±0.5	12.5±1.2
	Chemical	5.1±0.2	7.8±0.3	10.5±0.4	14.2±0.4	17.3±0.5	25.0±2.1
Pseudomonas aeruginosa	Green	9.4±0.4	12.8±0.5	16.7±0.5	20.3±0.5	24.5±0.6	10.0±0.9
	Chemical	5.8±0.3	8.5±0.4	11.9±0.4	15.8±0.5	19.2±0.5	20.0±1.8
Staphylococcus aureus	Green	10.1±0.4	13.9±0.5	18.0±0.5	22.1±0.5	26.3±0.6	8.0±0.7
	Chemical	6.2±0.3	9.1±0.4	12.5±0.4	16.5±0.5	20.1±0.5	16.0±1.5
Klebsiella pneumoniae	Green	8.9±0.3	12.1±0.4	15.8±0.5	19.7±0.4	23.5±0.5	12.5±1.1
	Chemical	4.9±0.2	7.5±0.3	10.2±0.4	13.9±0.4	17.0±0.5	25.0±2.0
Salmonella enterica Typhimurium	Green	7.8±0.3	10.5±0.4	14.0 0.4	17.9±0.4	21.4±0.5	15.0±1.3
	Chemical	4.5±0.2	6.8±0.3	9.3±0.3	12.6±0.4	15.8±0.4	30.0±2.5
Enterococcus faecalis	Green	7.2±0.3	9.8±0.4	13.1±0.4	16.8±0.4	20.2±0.5	18.0±1.5
	Chemical	4.1±0.2	6.2±0.3	8.5±0.3	11.5±0.4	14.7±0.4	35.0±2.8
Bacillus cereus	Green	6.5±0.3	8.9±0.4	11.9±0.4	15.4±0.5	18.9±0.5	20.0±1.7
	Chemical	3.7±0.2	5.6±0.3	7.8±0.3	10.3±0.4	13.4±0.4	40.0±3.0
Acinetobacter baumannii	Green	9.8±0.4	13.2±0.5	17.3±0.5	21.0±0.5	25.1±0.6	10.0±0.8
	Chemical	5.5±0.3	8.2±0.4	11.4±0.4	14.7±0.5	18.3±0.5	22.0±1.9

Values expressed as mean ± SE (n = 3). Data analyzed by two-way ANOVA (factors: nanoparticle type, concentration) followed by Tukey's post hoc test; P<0.05 considered significant

was the most susceptible (MIC 8.0 µg/mL), while *Bacillus cereus* showed relative tolerance (MIC 20.0 µg/mL). This broad-spectrum efficacy encompassed both Gram-positive strains *(E. faecalis* VRE) and notoriously resistant Gram-negative pathogens *(E. coli*, *K. pneumoniae*, *P. aeruginosa*, *A. baumannii)*. The mean ZOI difference between green and chemical AgNPs increased from 3.2 mm to 5.1 mm across the concentration gradient, unequivocally demonstrating that phytochemical capping agents enhance membrane disruption and intracellular ROS generation, yielding superior bactericidal outcomes.

Anticancer Activity: Against HCT-116 human colon adenocarcinoma cells, green-synthesized AgNPs exhibited an IC_{50} of 12.4 µg/mL, making them approximately 2.3-fold more potent than chemically synthesized AgNPs, which showed an IC_{50} of 28.6 µg/mL *(Table 3; Fig. 4)*. At 20 µg/mL, green AgNPs reduced viability to 58.3%, versus 82.5% for chemical; at 80 µg/mL, they nearly eradicated the population (14.2% viability), while chemical AgNPs left 41.8% intact. Mechanistically, this profound cytotoxicity is anchored in the intrinsic mitochondrial apoptotic pathway. Green AgNPs triggered a 4.8-fold surge in Caspase-3 activity, compared to a mere 2.1-fold increase induced by chemical AgNPs. Western blot analyses revealed that Bcl-2 was suppressed to 28.5% of control levels by green AgNPs, versus 61.3% by chemical, while Bax was upregulated to 312% of control, compared to 175% by chemical. This generated a massively elevated Bax/Bcl-2 ratio of 10.9, effectively lowering the apoptotic threshold, versus only 2.9 for chemical AgNPs. Flow cytometry quantified total apoptosis at 42.6% for green AgNPs-more than double the 18.3% observed for chemical confirming robust and selective engagement of the mitochondrial death cascade.

Growth Performance and Tumor-related Parameters: In the MNU-induced colon carcinogenesis rat model, the untreated cancer group developed severe cachexia, characterized by body weight gain of merely 15.4% (versus 95.6% in healthy controls), a 44% reduction in food intake, and 50% mortality by week 12 *(Table 4)*. Administration of green AgNPs at 80, 160, and 320 mg/kg effectuated a striking, dose-dependent reversal of this wasting syndrome. At 320 mg/kg, green AgNPs achieved weight gain (78.6%) and food intake statistically indistinguishable from healthy controls, with zero mortality. When directly compared at an equivalent dose (320 mg/kg), green AgNPs

Table 3. *Anticancer activity of green vs. chemical AgNPs against colon cancer cells*

Parameter	Green AgNPs (Mean ± SE)	Chemical AgNPs (Mean ± SE)
IC_{50} (µg/mL) - 48 h	12.4±1.1	28.6±2.3
Cell viability at 20 µg/mL (%)	58.3±2.1	82.5±2.8
Cell viability at 40 µg/mL (%)	31.7±1.9	64.2±2.5
Cell viability at 80 µg/mL (%)	14.2±1.2	41.8±2.1
Cell viability at 160 µg/mL (%)	6.8±0.7	26.5±1.9
Cell viability at 320 µg/mL (%)	2.1±0.3	14.3±1.2
Caspase-3 activity (fold change vs. control) - at IC_{50} conc.	4.8±0.4	2.1±0.2
Caspase-3 activity at 160 µg/mL	6.5±0.5	3.4±0.3
Caspase-3 activity at 320 µg/mL	7.9±0.6	4.2±0.4
Bcl-2 expression (% of control) - at IC_{50} conc.	28.5±2.2	61.3±3.1
Bcl-2 expression at 160 µg/mL (% of control)	15.2±1.5	42.6±2.8
Bcl-2 expression at 320 µg/mL (% of control)	7.8±0.9	28.4±2.1
Bax expression (% of control) - at IC_{50} conc.	312±18	175±12
Bax expression at 160 µg/mL (% of control)	415±22	238±15
Bax expression at 320 µg/mL (% of control)	487±25	291±18
Bax/Bcl-2 ratio - at IC_{50} conc.	10.9±0.9	2.9±0.3
Bax/Bcl-2 ratio at 160 µg/mL	27.3±2.1	5.6±0.5
Bax/Bcl-2 ratio at 320 µg/mL	62.4±4.5	10.2±0.9
Apoptotic cells (% by flow cytometry) - at IC_{50} conc.	42.6±2.5	18.3±1.7
Apoptotic cells at 160 µg/mL (%)	61.8±3.2	31.4±2.2
Apoptotic cells at 320 µg/mL (%)	78.5±3.8	45.2±2.9

Values expressed as mean ± SE (n=3). Data analyzed by two-way ANOVA (factors: nanoparticle type, concentration) followed by Tukey's post hoc test; P<0.05 considered significant

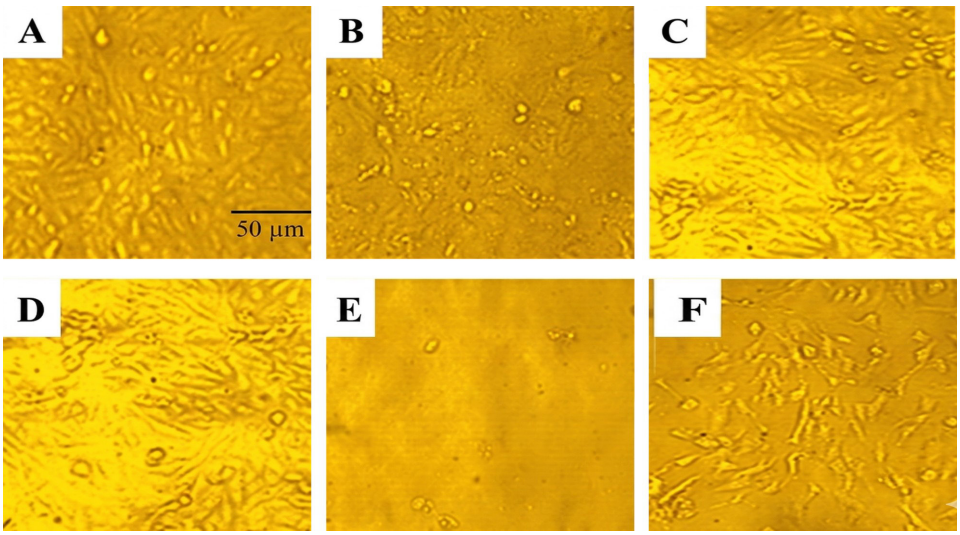

Fig 4. Comparative analysis of silver nanoparticle anti-cancer efficacy against HCT-116 colon cancer cells. Photomicrographs (A-F) show stained HCT-116 colon cancer cells under various treatment conditions. (**A**) Control cell line, exhibiting high cell viability and confluency with normal cellular structure. (**B**) Cells treated with 160 µg/mL Chemical AgNPs. **C:** Cells treated with 320 µg/mL Chemical AgNPs. Both B and C demonstrate dose-dependent effects on cell viability, with a clear reduction in cell number. (**D**) Cells treated with 160 µg/mL Green AgNPs. (**E**) Cells treated with 320 µg/mL Green AgNPs. D and E show significantly greater efficacy in reducing cell viability compared to equivalent chemical AgNP doses. (**F**) Cells treated with Doxorubicin (positive control), showing extensive cell death and characteristic changes in morphology consistent with effective anti-cancer therapy. The 50 µm scale bar is indicated in panel A

consistently outperformed chemical AgNPs, which were associated with 16.7% mortality and inferior weight gain (63.7%). Tumor-related parameters fully supported this: green AgNPs at 320 mg/kg reduced tumor incidence to 16.7% (vs. 50% for chemical), decreased average tumor size to 22 mm^3 (vs. 68 mm^3), lowered multiplicity to 0.5 tumors/rat (vs. 1.5), and improved histopathological scores to 0.9, indicating mild dysplasia (vs. 1.8 for chemical). Crucially, in a prophylactic setting where administration commenced concurrently with MNU, green AgNPs completely prevented tumor development (0% incidence, 0% mortality) and preserved near-normal histology (score 0.2), whereas chemical AgNPs still permitted 33.3% incidence and 16.7% mortality *(Table 5)*.

***Table 4**. The comparative effect of green and chemical silver nanoparticles at three concentrations (80, 160, and 320 mg/kg diet) on the growth parameters and mortality of MNU-induced colon cancer in rats*

Treatment	Description	Initial Body Weight (g)	Final Body Weight (g)	Body Weight Gain (%)	Food Intake (g/day)	Feed Efficiency Ratio (FCR)	Mortality (%)	Survival Rate (%)
T1	Healthy control (no MNU, no treatment)	180±5.2	352±8.1	95.6±3.2	22.4±0.8	0.32 ±0.02	0	100
T2	MNU-induced colon cancer, no treatment	182±4.8	210±6.5***	15.4±1.8***	12.6±0.6***	0.09±0.01***	50	50
T3	MNU + Green AgNPs (80 mg/kg)	181±5.0	248±7.2*	37.0±2.5*	15.8±0.7*	0.16±0.02*	33.3	66.7
T4	MNU + Green AgNPs (160 mg/kg)	183±4.9	288±7.8**	57.4±3.1**	18.5±0.8**	0.23±0.02**	16.7	83.3
T5	MNU + Green AgNPs (320 mg/kg)	182±5.1	325±8.2**	78.6±3.5**	21.2±0.9**	0.29±0.02**	0	100
T6	MNU + Chemical AgNPs (80 mg/kg)	181±4.7	228±6.9	26.0±2.2	14.1±0.6	0.12±0.01	41.7	58.3
T7	MNU + Chemical AgNPs (160 mg/kg)	184±5.0	258±7.4	40.2±2.8	16.5±0.7	0.18±0.02	33.3	66.7
T8	MNU + Chemical AgNPs (320 mg/kg)	182±4.9	298±7.9	63.7±3.2	19.3±0.8	0.25±0.02	16.7	83.3
T9	MNU + Green AgNPs (320 mg/kg) *- preventive*	183±5.2	341±8.5**	86.3±3.7**	21.8±0.9**	0.31±0.02**	0	100
T10	MNU + Chemical AgNPs (320 mg/kg) *- preventive*	182±5.0	312±8.0	71.4±3.4	20.1±0.8	0.27±0.02	16.7	83.3

*Values expressed as mean ± SE (n=3). Data analyzed by two-way ANOVA (factors: nanoparticle type, concentration) followed by Tukey's post hoc test; P<0.05; ** P<0.01; *** P<0.001 (one-way ANOVA with Tukey's post-hoc) considered significant*

***Table 5**. The effect of green and chemical AgNPs on Tumor-related parameters in MNU-induced colon cancer in rats (at study end, week 12)*

Treatment Group	Tumor Incidence (%)	Average Tumor Size (mm^3)	Tumor Multiplicity (n/rat)	Colon Histopathology Score (0-4)
T1 (Control)	0	0±0	0±0	0±0
T2 (MNU only)	100	285±32	4.8±0.6	3.8±0.2
T3 (Green 80)	83.3	156±21*	3.2±0.5*	2.9±0.3*
T4 (Green 160)	50.0	78±14**	1.8±0.4**	2.1±0.2**
T5 (Green 320)	16.7	22±6**	0.5±0.2**	0.9±0.2**
T6 (Chemical 80)	100	214±28	4.1±0.6	3.4±0.3
T7 (Chemical 160)	83.3	142±19	3.0±0.5	2.7±0.3
T8 (Chemical 320)	50.0	68±12*	1.5±0.3*	1.8±0.2*
T9 (Green preventive 320)	0	0±0**	0±0**	0.2±0.1**
T10 (Chemical preventive 320)	33.3	42±9	1.0±0.3	1.2±0.2

*Values expressed as mean ± SE (n=3). Data analyzed by two-way ANOVA (factors: nanoparticle type, concentration) followed by Tukey's post hoc test; P<0.05; ** P<0.01; *** P<0.001 (one-way ANOVA with Tukey's post-hoc) considered significant*

Oxidative Stress Markers: The oxidative stress data provide key mechanistic insights. The MNU-only group exhibited a profound imbalance, with malondialdehyde (MDA) and nitric oxide (NO) rising nearly 5-fold and 4.6-fold, respectively, indicating extensive lipid peroxidation and nitrosative stress *(Table 6)*. Concomitantly, endogenous antioxidant enzymes SOD, CAT, and GSH fell by approximately two-thirds, and total antioxidant capacity (TAC) declined by 66%. Administration of green AgNPs produced a clear dose-dependent restoration; at 320 mg/kg, all oxidative markers were restored to within 7-10% of normal values, and TAC reached 93% of the control level. At equivalent doses, green AgNPs consistently outperformed chemical AgNPs, yielding lower MDA/NO and higher SOD/CAT/GSH/TAC. This superiority is mechanistically attributed to the phytochemical coating, which facilitates direct radical scavenging, activates the Nrf2-driven transcriptional upregulation of endogenous antioxidant enzymes, inhibits pro-oxidant systems like NADPH oxidase, and chelates metal ions features absent in bare chemical AgNPs.

***Table 6.** Effect of green vs. chemical AgNPs on oxidative stress markers in MNU-induced colon cancer rats*

Treatment	Description	MDA (nmol/mg protein)	SOD (U/mg protein)	CAT (U/mg protein)	GSH (µmol/mg protein)	NO (µmol/mg protein)	TAC (mmol/L)
T1	Healthy control (no MNU, no treatment)	1.8±0.2	28.5±1.8	22.3±1.5	12.6±0.9	2.1±0.2	1.85±0.12
T2	MNU-induced colon cancer, no treatment	8.4±0.6***	9.2±0.8***	7.5±0.6***	3.8±0.3***	9.6±0.7***	0.62±0.05***
T3	MNU + Green AgNPs (80 mg/kg)	6.1±0.5*	14.8±1.2*	11.9±0.9*	5.9±0.5*	7.2±0.6*	0.94±0.07*
T4	MNU + Green AgNPs (160 mg/kg)	4.2±0.4**	20.1±1.5**	16.8±1.2**	8.7±0.7**	4.5±0.4**	1.35±0.09**
T5	MNU + Green AgNPs (320 mg/kg)	2.5±0.3**	26.4±1.9**	21.0±1.4**	11.5±0.9**	2.8±0.3**	1.72±0.11**
T6	MNU + Chemical AgNPs (80 mg/kg)	7.1±0.5	11.5±1.0	9.2±0.7	4.8±0.4	8.3±0.6	0.78±0.06
T7	MNU + Chemical AgNPs (160 mg/kg)	5.6±0.4	16.2±1.3	13.5±1.0	6.7±0.5	6.1±0.5	1.08±0.08
T8	MNU + Chemical AgNPs (320 mg/kg)	3.9±0.4*	22.3±1.6*	18.4±1.3*	9.5±0.7*	3.9±0.4*	1.48±0.10*
T9	MNU + Green AgNPs (320 mg/kg) – *preventive*	1.9±0.2**	27.9±2.0**	22.0±1.6**	12.3±0.9**	2.2±0.2**	1.82±0.12**
T10	MNU + Chemical AgNPs (320 mg/kg) – *preventive*	3.1±0.3	24.1±1.7	19.8±1.4	10.4±0.8	3.2±0.3	1.58±0.11

*P<0.05; ** P<0.01; *** P<0.001 (one-way ANOVA with Tukey's post-hoc) MDA = malondialdehyde (lipid peroxidation marker); SOD = superoxide dismutase; CAT = catalase; GSH = reduced glutathione; NO = nitric oxide; TAC = total antioxidant capacity. Tissue analyzed: Colon mucosa homogenate. Values: Mean ± SE (n = 6 rats per group). MNU induction: Single intrarectal dose (30 mg/kg) at week 0. Treatments: Daily oral gavage for 12 weeks*

Histology of Colon Tissues: H&E-stained sections provided a visual narrative aligned impeccably with the biochemical data. Healthy controls *(Fig. 5-A)* displayed well-organized crypts, intact epithelium, and abundant goblet cells. The MNU-only group *(Fig. 5-B)* exhibited severe disruption, fragmented crypts, extensive goblet cell loss, and robust inflammatory infiltration. Therapeutic chemical AgNPs *(Fig. 5-C)* offered only moderate restoration, with partially regenerated crypts but persistent residual inflammation. In stark contrast, therapeutic green AgNPs *(Fig. 5-D)* revealed near-normal crypt morphology with abundant goblet cells and only mild residual inflammatory foci. Preventive chemical AgNPs *(Fig. 5-E)* provided significant protection with well-aligned crypts and minimal inflammation, but it was the preventive green AgNPs group *(Fig. 5-F)* that exhibited the most profound histoprotection perfectly healthy crypts, abundant goblet cells, and a complete absence of inflammatory infiltrate. This histological progression unequivocally demonstrates that green-synthesized AgNPs are superior in both therapeutic and preventive settings, confirming that their anticancer mechanisms involve effective oxidative stress mitigation and mucosal integrity preservation.

Discussion

Green nanotechnology is gaining momentum as researchers seek safer, more biocompatible, and environmentally responsible alternatives to conventionally synthesized nanomaterials. Traditional chemical routes for AgNPs production often rely on harsh reducing agents and organic solvents, leaving residual contaminants on particle surfaces that can compromise biocompatibility and raise concerns about cytotoxicity and systemic toxicity in clinical use, especially for vulnerable groups such as cancer patients.

By contrast, green or bioinspired synthesis employs biological systems-plants, bacteria, fungi, algae, or purified biomolecules, as intrinsic reducing and capping agents, thereby avoiding hazardous reagents and significantly lowering the ecological footprint of nanoparticle production [19]. In this study, the choice of purslane extract as a "bionanofactory" is in line with this approach: microbial enzymes, peptides, and metabolites simultaneously drive metal-ion reduction and surface capping, yielding AgNPs with improved colloidal stability, narrower size distributions, and biologically active surface coronas [20]. Such biomolecular coatings have been shown to enhance antimicrobial and anticancer performance while dampening offtarget toxicity, largely by improving hemocompatibility and reducing nonspecific damage to normal mammalian cells. This safety dimension is particularly critical when AgNPs are envisioned for longterm chemoprevention or as adjuvants alongside cytotoxic cancer drugs [21].

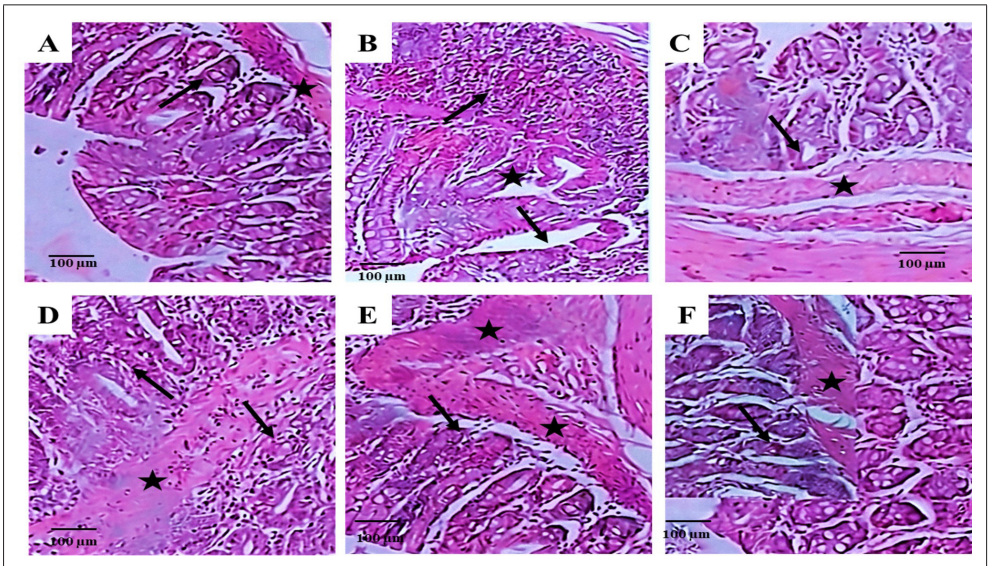

Fig 5. Histological assessment of rat colon tissue following MNU induction and AgNPs treatments. Photomicrographs (A-F) show H&E-stained sections of rat colon (magnification X400). Pointers indicate notable pathological features. **(A)** Control Group: Exhibiting normal tissue architecture with well-organized crypts and intact mucosal layers. **(B)** MNU-Treated Rats (Untreated): Showing significant disruption of crypt architecture, loss of goblet cells, and signs of inflammatory cell infiltration. **(C)** MNU + Chemical AgNPs (320 mg/kg): Demonstrating moderate restoration of tissue structure with a visible increase in goblet cells compared to the untreated MNU group. **(D)** MNU + Green AgNPs (320 mg/kg): Revealing substantial tissue repair with near-normal crypt morphology and abundant regenerated goblet cells. **(E)** MNU + Chemical AgNPs (Preventative): Displaying significant protection against MNU-induced damage, with tissue architecture resembling the control group. **(F)** MNU + Green AgNPs (Preventative): Exhibiting excellent preventative effects, maintaining healthy tissue structure and abundant goblet cells, similar to the control

Multiple comparative studies indicate that greensynthesized AgNPs exhibit stronger antioxidant activity than chemically synthesized AgNPs at comparable doses, and this aligns with the current findings. In a direct comparison using *Mussaenda frondosa* extract vs sodium citrate, green AgNPs showed "remarkable antioxidant activity" in the DPPH assay, clearly surpassing chemically synthesized AgNPs and being highlighted as preferable for biomedical use [22]. A second comparative study using *Cassia fistula* also reported higher antioxidant activity for green AgNPs (84.48% vs 75.87% for chemical AgNPs) and a lower IC_{50} for the green formulation, indicating more efficient radical scavenging at lower concentrations [23]. Mechanistically, this superiority is attributed to phytochemical capping layers (polyphenols, flavonoids, tannins, alkaloids) on green AgNPs, which provide additional redoxactive sites and stabilize surface electrons, enhancing radical scavenging compared with citratecapped or chemically reduced AgNPs that lack these bioactive shells [24].

Green-synthesized AgNPs, which show larger ZOIs and ~2-fold lower MICs than chemical AgNPs, are strongly supported by comparable studies. In this regard, Barabadi et al.[25] prepared plant-mediated AgNPs from *Zataria multiflora* and directly compared them to commercial AgNPs against *S. aureus*. Green AgNPs were roughly twice as potent, with an MIC of 4 µg/mL versus 8 µg/mL for commercial particles, and also displayed superior biofilm inhibition, especially at sub-MIC levels. This mirrors the two-fold MIC reduction and enhanced ZOIs observed in our data, particularly for *S. aureus*.

Several comparative or review studies conclude that green AgNPs generally outperform chemically synthesized AgNPs at the same or lower doses. A recent systematic review of green-synthesized, bio-capped AgNPs against multidrug-resistant bacteria reports MICs as low as 2.5 µg/mL, ZOIs up to 25 mm, and emphasizes that capping by plant/bacterial metabolites synergistically enhances antibacterial activity compared with "bare" or simply polymer-stabilized chemical AgNPs [26]. They achieve this primarily by utilizing metal nanoparticle mechanisms, such as cell membrane disruption and reactive oxygen species (ROS) generation, to effectively bypass traditional bacterial resistance pathways in a head-to-head test of green vs chemically produced AgNPs against *Salmonella typhi*, *Bacillus cereus*, and *Pseudomonas aeruginosa*, and likewise reported consistently higher antimicrobial efficacy for green particles [27-29].

More mechanistic comparisons support our interpretation that particle size, surface chemistry, and phytochemical capping explain the superior activity. A focused comparison on *S. aureus* found that greensynthesized AgNPs from Cassia seed or green tea had MICs of 5-25 µg/mL, significantly lower than citrate or $NaBH_4$ reduced AgNPs of similar size; antibacterial potency correlated inversely with size but remained higher for green AgNPs even when size was controlled [30].

The ranking of susceptibility in the study, with *S. aureus* among the most sensitive strains and some Gram-positive and Gram-negative species more tolerant, is consistent with the variable MIC ranges reported for green AgNPs. Sahu et al.[31] found that green AgNPs synthesized using citrus extract had substantially lower MICs than chemically synthesized AgNPs against both *S. aureus* and *E. coli* (~46-50 vs 77-87 µg/mL), again paralleling our ~2fold MIC advantage.

Green AgNPs show dosedependent, significantly superior antimicrobial activity compared with chemically synthesized AgNPs with roughly twofold lower MICs and larger ZOIs across diverse pathogens is in strong agreement with the broader literature, which attributes this to smaller particle size, higher surface reactivity, and synergistic phytochemical capping [26].

Green-synthesized silver nanoparticles (AgNPs) using purslane extract, which show markedly greater cytotoxicity and apoptosis in HCT116 cells than chemically synthesized AgNPs, are highly consistent with broader findings on green AgNPs in colon cancer models. Multiple studies report low micromolar IC_{50} values for plant-mediated AgNPs against HCT116 and other colorectal lines, often markedly lower than either the corresponding plant extract or a simple silver salt, reflecting synergistic effects between the metal core and the phytochemical capping layer [32]. For example, Marine algal AgNPs from *Chaetomorpha linum* and *Ulva lactuca* showed clear dosedependent cytotoxicity toward HCT116, with selective toxicity over normal colon epithelial cells and mechanistic signatures similar to our work: upregulation of proapoptotic Bax, p53, caspase3/9, and Bid, and downregulation of antiapoptotic Bcl2/Bclxl, indicating mitochondrial (intrinsic) apoptosis as the dominant pathway [33].

The marked shift in the Bax/Bcl-2 ratio and robust caspase-3 activation observed with purslane AgNPs parallel these reports. Green-synthesized *Moringa oleifera* and *Adansonia digitata* AgNPs also showed pronounced, dose-dependent killing of HCT-116 and other colon lines and modulation of key survival pathways (Wnt/β-catenin components CTNNB1, APC, LRP5/6), consistent with profound interference in proliferative signaling [34]. A recent review on green AgNPs in colon cancer highlights that, compared with chemically synthesized particles, green AgNPs generally achieve greater reductions in cell viability at lower doses, with better selectivity toward tumor over normal cells, largely via ROS-mediated mitochondrial apoptosis and p53-linked pathways [35].

Although explicit headtohead comparisons with a chemically

synthesized AgNPs control are rare, greensynthesized AgNPs frequently outperform metal salt, plant extract alone, or polymercapped AgNPs at equivalent or lower concentrations, and induce higher caspase activity and more extensive apoptosis [36]. The approximately 2fold lower IC_{50} of purslaneAgNPs compared with chemical AgNPs and the stronger activation of caspase3 and Bax, with greater Bcl2 suppression and higher apoptotic fractions, therefore fits well into a broader pattern where plantcapped AgNPs show enhanced potency and efficacy in colorectal cancer models, likely due to smaller size, improved stability, and cooperative effects of codelivered phytochemicals.

The present findings concern an MNU induced colorectal cancer model treated with green versus chemical AgNPs, focusing on growth performance/feed efficiency *(Table 4)* and tumor burden/multiplicity and histopathology *(Table 5)*. No prior work was found using exactly the same model and formulations, but several lines of evidence from other species and tumor types are relevant.

The marked reductions in tumor incidence, size, multiplicity, and dysplasia score with green AgNPs *(Table 5)* align with general oncologic observations that smaller, fewer, and lowergrade tumors are associated with better outcomes. In intrahepatic cholangiocarcinoma, tumor multiplicity is an independent adverse prognostic factor; patients with multiple tumors have survival similar to those with more advanced stage disease, leading authors to call for multiplicity to be explicitly weighted in staging systems [37]. For hepatocellular carcinoma, tumor size strongly predicts microscopic vascular invasion and high histologic grade, with lesions >5 cm having substantially higher rates of occult vascular invasion and poor differentiation than smaller tumors [38]. Analogous relationships between size and aggressive histology are seen in welldifferentiated thyroid cancer, where larger tumors show worse survival, particularly when combined with other highrisk features [39].

Histopathologic scoring systems in other tumor types (adipose and phyllodes tumors) similarly demonstrate that increasing grades of atypia, mitotic activity, and necrosis correlate with more aggressive biological behavior and worse prognosis [40]. Within this context, the shift from multiple, larger tumors with moderate dysplasia in MNU-only or chemically treated rats to fewer, smaller lesions with largely mild dysplasia under green AgNPs treatment, as shown in *Table 6*, is consistent with a genuine reduction in malignant potential rather than merely a cytostatic delay. This robust tumor suppression is strongly linked to the high concentration of plant polyphenols capping the green AgNPs, which have been independently shown to effectively manage and prevent colorectal cancer in rodent models [41].

Green AgNPs effectively mitigate MNU-induced oxidative damage in colon tissue and outperform chemically synthesized AgNPs, yielding near-complete redox and tumor protection. This aligns with extensive evidence that green AgNPs exert anticancer effects via redox modulation and apoptosis. Naringenin-capped AgNPs, are highly cytotoxic to HCT116 cells, increasing ROS/MDA, impairing ATP, triggering p53-mediated apoptosis and cell-cycle arrest, with transcriptomic enrichment of oxidation-reduction pathways [42]. Nostocsynthesized AgNPs against HCT116 and other cancer lines via oxidative stress and p53/caspase3 activation, and a range of plantmediated AgNPs are summarized in recent mechanistic and review articles [43]. A focused review on greensynthesized AgNPs for colon cancer further concludes that these particles typically induce ROS and mitochondrial dysfunction in tumor cells while showing improved biocompatibility and selective cytotoxicity relative to chemical AgNPs [35]. Collectively, these sources support the idea that green AgNPs can both protect normal tissue and attack malignant cells through contextdependent redox modulation.

The bidirectional redox behavior observed here, antioxidant in normal colon while antitumor in cancer, is also mirrored in other *in vivo* models. Chlorogenic acid–BSA AgNPs in lymphoma-bearing mice enhanced host antioxidant defenses (↑GSH, SOD, CAT, GPx; ↓MDA) while reducing tumor burden, similar to the normalization of TAC and enzyme activities observed with higher doses of green AgNPs in the current colon model [44]. In contrast, Nostoc-synthesized AgNPs selectively increased oxidative stress within tumor cells and activated p53 and caspase-3, yet spared systemic parameters, suggesting that green AgNPs can drive tumors toward lethal oxidative imbalance while maintaining host redox homeostasis [45]. Toxicological work in healthy rats shows that coating chemistry is critical: ethylene glycol AgNPs increased TAC and CAT and lowered TBARS, whereas PVP-coated AgNPs decreased GSH and TAC and increased protein carbonyls, demonstrating that surface functionalization dictates whether AgNPs shift the organism toward an antioxidant or pro-oxidant state [46]. This is consistent with broader reviews documenting that plantderived capping layers rich in polyphenols and flavonoids confer more favorable redox and safety profiles than many chemically coated formulations [8].

The present study introduces several novel elements. Most colondirected AgNPs research has been *in vitro* (HCT116, DLD1, SW480) with a focus on ROSmediated cytotoxicity and apoptosis, often without parallel evaluation of effects on normal tissue [43]. *In vivo* studies demonstrating enhancement of systemic antioxidant capacity and tumor suppression exist but typically do not directly compare

green and chemically synthesized AgNPs or quantify detailed redox-tumor correlations in a colonspecific carcinogenesis model [14]. By directly contrasting green and chemical AgNPs at matched doses, the current work extends coatingdependent redox phenomena described in toxicology models [46] into a colon carcinogen setting. The quantitative linkage between oxidative markers (MDA, TAC) and tumor size, multiplicity, body weight, and mortality also extends beyond the more inferential associations reported earlier [14]. Finally, the demonstration that prophylactic green AgNPs can almost completely prevent carcinogen-induced oxidative stress and colon tumor formation, whereas therapeutic dosing only partially reverses established lesions, addresses an early-versus-lateintervention question that has rarely been explored in AgNPs colon cancer research.

The chemopreventive and therapeutic effects of green AgNPs on MNU-induced colorectal carcinogenesis align with numerous studies on plant-mediated AgNPs in colon cancer. Multiple reports show green AgNPs exert potent, selective cytotoxicity against colorectal cancer cell lines (HCT116, HT29, Caco-2, etc.) while sparing normal cells, mirroring the tumor suppression and safety observed in our colon histology [36]. For example, pectinstabilized AgNPs showed strong cytotoxicity toward several human colorectal lines with minimal toxicity to HUVECs [47], consistent with our study.

The *in vivo* superiority of green over chemical AgNPs parallels other models, with lower toxicity. Croton tiglium AgNPs in AOM-induced colon cancer improved oxidative/inflammatory markers and histopathology, supporting a generalizable chemopreventive/therapeutic role [48].

This study confirms that purslane-derived green AgNPs are safe, eco-friendly, and potent with dual antimicrobial and anticancer applications. The sustainable synthesis avoids toxic agents and yields favorable physicochemical properties. These findings support green AgNPs as chemopreventive/adjunctive agents for colon cancer and as antimicrobials against multidrug-resistant pathogens, underscoring the value of biologically driven nanofabrication.

Declarations

Availability of Data and Materials: The datasets and analyzed during the current study available from the corresponding author (ASA) on reasonable request.

Ethical Statement: The animal study has been reviewed and approved by ZU-IACUC committee. was performed in accordance with the guidelines of the Egyptian Research Ethics Committee and the guidelines specified in the Guide for the Care and Use of Laboratory Animals (2023). Ethical code number ZU-IACUC/2/F/313/2023.

Funding Support: This research was funded by Princess Nourah bint Abdulrahman University Researchers Supporting Project number (PNURSP2026R461), Princess Nourah bint Abdulrahman University, Riyadh, Saudi Arabia Deanship of Research and Graduate Studies at King Khalid University for funding work through the Large Research Project under grant number RGP.2/586/46.

Acknowledgment: The authors gratefully acknowledge Princess Nourah bint Abdulrahman University Researchers Supporting Project number (PNURSP2026R461), Princess Nourah bint Abdulrahman University, Riyadh, Saudi Arabia. The authors extend their appreciation to the Deanship of Research and Graduate Studies at King Khalid University for funding work through the Large Research Project under grant number RGP.2/586/46.

Conflict of Interest: The authors declare that they have no conflicts of interest. All authors have given their consent that this work is valid and represent their views of the study and have given their consent for this work to be published.

Declaration of Generative Artificial Intelligence (AI): The authors declare that the article, tables and figures were not written/created by AI and AI-assisted Technologies.

Author Contributions: Conceptualization, ASA, SSM, AMA, KMA, and KAM, formal analysis, MAA, AOS, AMA, MOA, and SAA, investigation, ASA, SSM, AMA, KMA, and KAM, data curation, MAA, AOS, AMA, MOA, SMAB, and MAA, writing original draft preparation, ASA, SSM, AMA, KMA, and KAM, writing final manuscript and editing, MAA, AOS, AMA, MOA, SMAB, and MAA, visualization and methodology, ASA, SSM, AMA, KMA, KAM, MAA, AOS, AMA, MOA, SMAB, and MAA. All authors have read and agreed to the published version of the manuscript.

References

1. **Dawadi S, Katuwal S, Gupta A, Lamichhane U, Thapa R, Jaisi S, Lamichhane G, Bhattarai D, Parajuli N:** Current research on silver nanoparticles: Synthesis, characterization, and applications. *J Nanomater,* 2021:6687290, 2021. DOI: 10.1155/2021/6687290
2. **Duman H, Eker F, Akdaşçi E, Witkowska A, Bechelany M, Karav S:** Silver nanoparticles: A comprehensive review of synthesis methods and chemical and physical properties. *Nanomaterials,* 14 (18):1527, 2024. DOI: 10.3390/Nano14181527
3. **Bamal D, Singh A, Chaudhary G, Kumar M, Singh M, Rani N, Mundlia P, Sehrawat A:** Silver nanoparticles biosynthesis, characterization, antimicrobial activities, applications, cytotoxicity and safety issues: An updated review. *Nanomaterials,* 11 (8):2086, 2021. DOI: 10.3390/nano11082086
4. **Abuzeid H, Julien C, Zhu L, Hashem A:** Green synthesis of nanoparticles and their energy storage, environmental, and biomedical applications. *Crystals,* 13 (11):1576, 2023. DOI: 10.3390/cryst13111576
5. **Hamouda R, Hussein M, Abo-Elmagd R, Bawazir S:** Synthesis and biological characterization of silver nanoparticles derived from the cyanobacterium *Oscillatoria limnetica*. *Sci Rep,* 9:13071, 2019. DOI: 10.1038/s41598-019-49444-y
6. **Sadan M, Almundarij R, Haridy M, EL-Khodery S, Elzarei MF, Abo-Aziza FAM, Ibrahim ZH, Abdellatif AAH:** Can Silver nanoparticles stabilized by Shilajit *(Asphaltum punjabianum)* accelerate tibial bone defects repair in rabbits: A preliminary study. *Int J Vet Sci,* 14 (3): 512-519, 2025. DOI: 10.47278/journal.ijvs/2024.276
7. **AlGheffari HK, Aljahdali SM, Albalawi M, Obidan A, Binothman N, Aljadani M, Aldawood N, Alahmady NF, Alqahtani SS, Alkahtani AM, Allohibi A, Abu Al-Khair W, Wahdan KM, Bouqellah NA:** Mycogenic zinc nanoparticles with antimicrobial, antioxidant, antiviral, anticancer, and anti-alzheimer activities mitigate the aluminium toxicity in mice: Effects on liver, kidney, and brain health and growth performance. *Pak Vet J,* 44 (3): 763-775, 2024. DOI: 10.29261/pakvetj/2024.252

8. **Sati A, Ranade T, Mali S, Yasin HKA, Pratap A:** Silver nanoparticles (AgNPs): Comprehensive insights into bio/synthesis, key influencing factors, multifaceted applications, and toxicity- A 2024 update. *ACS Omega,* 10 (8): 7549-7582, 2025. DOI: 10.1021/acsomega.4c11045

9. **Alsamhary K:** Eco-friendly synthesis of silver nanoparticles by *Bacillus subtilis* and their antibacterial activity. *Saudi J Biol Sci,* 27 (8): 2185-2191, 2020. DOI: 10.1016/j.sjbs.2020.04.026

10. **Yu X, Li J, Mu DS, Zhang H, Liu Q, Chen G:** Green synthesis and characterizations of silver nanoparticles with enhanced antibacterial properties by secondary metabolites of *Bacillus subtilis* (SDUM301120). *Green Chem Lett Rev,* 14, 190-203, 2021. DOI: 10.1080/17518253.2021.1894244

11. **Xu J, Yıldıztekin M, Han D, Keskin C, Baran A, Baran MF, Eftekhari A, Ava CA, Kandemir Sİ, Cebe DB, Dağ B, Beilerli A, Khalilov R:** Biosynthesis, characterization, and investigation of antimicrobial and cytotoxic activities of silver nanoparticles using *Solanum tuberosum* peel aqueous extract. *Heliyon,* 9 (8):e19061, 2023. DOI: 10.1016/j.heliyon.2023.e19061

12. **Solís-Sandí I, Cordero-Fuentes S, Pereira-Reyes R, Vega-Baudrit JR, Batista-Menezes D, Montes de Oca-Vásquez G:** Optimization of the biosynthesis of silver nanoparticles using bacterial extracts and their antimicrobial potential. *Biotechnol Rep,* 40:e00816 2023. DOI: 10.1016/j.btre.2023.e00816

13. **Ali E, Abu-Hussien SH, Hesham E, Ahmed S, Mostafa H, Gamal A, El-Sayed SM, Hemdan B, Bakry A, Ebeed NM, Elhariry H, Galal A, Abd-Elhalim BT:** Compatibility and antimicrobial activity of silver nanoparticles synthesized using *Lycopersicon esculentum* peels. *AMB Express,* 14 (1):120, 2024. DOI: 10.1186/s13568-024-01774-5

14. **Wypij M, Jędrzejewski T, Trzcińska-Wencel J, Ostrowski M, Rai M, Golińska P:** Green synthesized silver nanoparticles: Antibacterial and anticancer activities, biocompatibility, and analyses of surface-attached proteins. *Front Microbiol,* 12:632505, 2021. DOI: 10.3389/fmicb.2021.632505

15. **Abada E, Habib F, Mashraqi A, Modafer Y, Alsolami W, Ismail K, Alamri A, Mashlawi A, Shater AR:** Eco-friendly synthesis and characterization of *Senna italica*-derived silver nanoparticles with broad-spectrum antimicrobial activity. *Int J Microbiol,* 2025:2072594, 2025, DOI: 10.1155/ijm/2072594

16. **Afrin S, Giampieri F, Forbes-Hernández TY, Gasparrini M, Amici A, Cianciosi D, Quiles JL, Battino M:** Manuka honey synergistically enhances the chemopreventive effect of 5-fluorouracil on human colon cancer cells by inducing oxidative stress and apoptosis, altering metabolic phenotypes and suppressing metastasis ability. *Free Radic Biol Med,* 126, 41-54, 2018. DOI: 10.1016/j.freeradbiomed.2018.07.014

17. **Poimenova I, Sozarukova M, Ratova DM, Nikitina V, Khabibullin V, Mikheev I, Proskurnina E, Proskurnin M:** Analytical methods for assessing thiol antioxidants in biological fluids: A review. *Molecules,* 29 (18):4433, 2024, DOI: 10.3390/molecules29184433

18. **Harshavardhini R, Dayanand G, Bheeshma B, Kumar OS:** A spectrum of colonic lesions in a study done at a tertiary care hospital, telangana. *Int J Multidiscip Res,* 8 (2): 1-19, 2024. DOI: 10.36948/ijfmr.2024.v06i05.28336

19. **Zehra SH, Ramzan K, Viškelis J, Viškelis P, Balčiūnaitienė A:** Advancements in green synthesis of silver-based nanoparticles: Antimicrobial and antifungal properties in various films. *Nanomaterials,* 15 (4):252, 2025, DOI: 10.3390/nano15040252

20. **Rónavári A, Igaz N, Adamecz D, Szerencsés B, Molnár C, Kónya Z, Pfeiffer I, Kiricsi M:** Green silver and gold nanoparticles: Biological synthesis approaches and potentials for biomedical applications. *Molecules,* 26 (4):844, 2021, DOI: 10.3390/molecules26040844

21. **Arshad F, Naikoo G, Hassan I, Chava S, El-Tanani M, Aljabali A, Tambuwala M:** Bioinspired and green synthesis of silver nanoparticles for medical applications: A green perspective. *Appl Biochem Biotechnol,* 196, 3636-3669, 2023, DOI: 10.1007/s12010-023-04719-z

22. **Sreelekha E, George B, Shyam A, Sajina N, Mathew B:** A comparative study on the synthesis, characterization, and antioxidant activity of green and chemically synthesized silver nanoparticles. *BioNanoSci,* 11, 489-496, 2021. DOI: 10.1007/s12668-021-00824-7

23. **Arland SE, Kumar J:** Green and chemical syntheses of silver nanoparticles: Comparative and comprehensive study on characterization, therapeutic potential, and cytotoxicity. *Eur J Med Chem Rep,* 11:100168, 2024. DOI: 10.1016/j.ejmcr.2024.100168

24. **Sarwer Q, Amjad M, Mehmood A, Binish Z, Mustafa G, Farooq A, Qaseem M, Abasi F, De La Lastra JP:** Green synthesis and characterization of silver nanoparticles using *Myrsine africana* leaf extract for their antibacterial, antioxidant and phytotoxic activities. *Molecules,* 27 (21):7612, 2022. DOI: 10.3390/molecules27217612

25. **Barabadi H, Mojab F, Vahidi H, Marashi B, Talank N, Hosseini O, Saravanan M:** Green synthesis, characterization, antibacterial and biofilm inhibitory activity of silver nanoparticles compared to commercial silver nanoparticles. *Inorg Chem Commun,* 129:108647, 2021. DOI: 10.1016/j.inoche.2021.108647

26. **Girma A, Alamnie G, Bekele T, Mebratie G, Mekuye B, Abera B, Workineh D, Tabor A, Jufar D:** Green-synthesised silver nanoparticles: Antibacterial activity and alternative mechanisms of action to combat multidrug-resistant bacterial pathogens: A systematic literature review. *Green Chem Lett Rev,* 17:108647, 2024, DOI: 10.1080/17518253.2024.2412601

27. **Hannan A, Du XX, Maqbool B, Khan A:** Nanoparticles as potent allies in combating antibiotic resistance: A promising frontier in antimicrobial therapy. *Pak Vet J,* 44 (4): 957-967, 2024. DOI: 10.29261/pakvetj/2024.227

28. **Batool S, Hashim M, Naseem F, Razzaq MF, Fakhar M, Khalid RUB, Ejaz H, Minal Z, Asad A, Khan AMA, Shakir MZ:** Mechanism and application of metal nanoparticles as antimicrobial agents. *Continental Vet J,* 5 (1): 93-102, 2025. DOI: 10.71081/cvj/2025.041

29. **Chahar V, Sharma B, Shukla G, Srivastava A, Bhatnagar A:** Study of antimicrobial activity of silver nanoparticles synthesized using green and chemical approach. *Colloids Surf A: Physicochem Eng Asp,* 554, 149-155, 2018, DOI: 10.1016/j.colsurfa.2018.06.012

30. **Secario MK, Truong T, Chen CC, Lai J, Lue S:** Exploring antibacterial effectiveness: A comparative analysis of green and chemical synthesis of silver nanoparticles against *Staphylococcus aureus. J Taiwan Inst Chem Eng,* 165:105750, 2024. DOI: 10.1016/j.jtice.2024.105750

31. **Sahu SK, Sahoo P, Dash S, Mishra SR, Behera PC:** Antimicrobial activity of silver nanoparticles against common bovine mastitis pathogens: A comparative analysis. *Curr Microbiol,* 82 (3):121, 2025. DOI: 10.1007/s00284-025-04101-8

32. **Zhai Y, Wang B, Han W, Yu B, Ci J, An F:** Green synthesis of AgNPs using plant extract and investigation of its anti-human colorectal cancer application. *Open Chem,* 21 (1):174, 2023. DOI: 10.1515/chem-2023-0174

33. **Acharya D, Satapathy S, Yadav K, Somu P, Mishra G:** Systemic evaluation of mechanism of cytotoxicity in human colon cancer HCT-116 cells of silver nanoparticles synthesized using marine algae *Ulva lactuca* extract. *J Inorg Organomet Polym Mater,* 32, 596-605, 2021. DOI: 10.1007/s10904-021-02133-8

34. **Khajeh H, Fazeli-Nasab B, Pourshahdad A, Mirzaei AR, Ghorbanpour M:** Green-synthesized silver nanoparticles induced apoptotic cell death in $CACO_2$ cancer cells by activating MLH1 gene expression. *Sci Rep,* 14:29601, 2024. DOI: 10.1038/s41598-024-80809-0

35. **Dohare S, Khandal J, Dongsar TS, Gupta G, Sahebkar A, Abourehab M, Kesharwani P:** Green-synthesized silver nanoparticles: A sustainable nanoplatform for targeted colon cancer therapy. *Int J Pharm,* 683:126015, 2025. DOI: 10.1016/j.ijpharm.2025.126015

36. **Bidian C, Filip GA, David L, Moldovan B, Olteanu D, Clichici S, Olănescu-Vaida-Voevod MC, Leostean C, Macavei S, Muntean DM, Cenariu M, Albu A, Baldea I:** Green synthesized gold and silver nanoparticles increased oxidative stress and induced cell death in colorectal adenocarcinoma cells. *Nanomaterials,* 13 (7):1251, 2023. DOI: 10.3390/nano13071251

37. **Yoon SJ, Park S, Kim H, Shin SH, Heo JS, Rhu J, Choi GS, Kim JM, Joh JW, Han IW:** The oncologic implications of tumor multiplicity

in intrahepatic cholangiocarcinoma: Its prognostic value might be underestimated. *Cancer Res Treat,* 55, 948-955, 2023. DOI: 10.4143/crt.2023.290

38. **Pawlik TM, Delman KA, Vauthey JN, Nagorney DM, Ng IO, Ikai I, Yamaoka Y, Belghiti J, Lauwers GY, Poon RT, Abdalla EK:** Tumor size predicts vascular invasion and histologic grade: Implications for selection of surgical treatment for hepatocellular carcinoma. *Liver Transplantation,* 11 (9): 1086-1092, 2005. DOI: 10.1002/lt.20472
39. **Ginzberg SP, Sharpe J, Passman JE, Amjad W, Wirtalla CJ, Soegaard Ballester JM, Finn CB, Mandel SJ, Kelz RR, Wachtel H:** Revisiting the relationship between tumor size and risk in well-differentiated thyroid cancer. *Thyroid,* 34 (8): 980-989, 2024. DOI: 10.1089/thy.2023.0327
40. **Deacu M, Bosoteanu M, Enciu M, Cozaru GC, Cojocaru O, Baltatescu GI, Nicolau AA, Orasanu CI, Caraban BM, Voda RI:** The predictive role of the histopathological scoring system in adipose tumors-lipoma, atypical lipomatous tumor, and liposarcoma. *Diagnostics,* 13 (24):3606, 2023. DOI: 10.3390/diagnostics13243606
41. **Gurunathan S, Qasim M, Park C, Yoo H, Kim JH, Hong K:** Cytotoxic potential and molecular pathway analysis of silver nanoparticles in human colon cancer cells HCT116. *Int J Mol Sci,* 19 (8):2269, 2018. DOI: 10.3390/ijms19082269
42. **Liu D, Huang L, Zhou Q, Meng Y:** Colorectal cancer management and prevention using plant polyphenols in the rodent models. *Pak Vet J,* 44 (3): 571-580, 2024. DOI: 10.29261/pakvetj/2024.231
43. **Khan MS, Alomari A, Tabrez S, Hassan I, Wahab R, Bhat SA, Alafaleq NO, Altwaijry N, Shaik GM, Zaidi SK, Nouh W, Alokail MS, Ismael MA:** Anticancer potential of biogenic silver nanoparticles: A mechanistic study. *Pharmaceutics,* 13 (5):707, 2021. DOI: 10.3390/pharmaceutics13050707
44. **Roy T, Dey S,K Pradhan A, Chaudhuri AD, Dolai M, Mandal SM, Choudhury SM:** Facile and green fabrication of highly competent surface-modified chlorogenic acid silver nanoparticles: Characterization and antioxidant and cancer chemopreventive potential. *ACS Omega,* 7, 48018-48033, 2022. DOI: 10.1021/acsomega.2c05989
45. **Hamida RS, Albasher G, Bin-Meferij MM:** Oxidative stress and apoptotic responses elicited by nostoc-synthesized silver nanoparticles against different cancer cell lines. *Cancers,* 12 (8):2099, 2020. DOI: 10.3390/cancers12082099
46. **Docea AO, Calina D, Buga AM, Zlatian O, Paoliello MMB, Mogosanu GD, Streba CT, Popescu EL, Stoica AE, Bîrcă AC, Vasile BŞ, Grumezescu AM, Mogoanta L:** The effect of silver nanoparticles on antioxidant/pro-oxidant balance in a murine model. *Int J Mol Sci,* 21 (4):1233, 2020. DOI: 10.3390/ijms21041233
47. **Wang D, Geng W, Li Q, Li G, Zhang D, Zhang H:** Ultrasonic green synthesis of silver nanoparticles mediated by pectin: Characterization and evaluation of the cytotoxicity, antioxidant, and colorectal carcinoma properties. *Arabian J Chem,* 15:103500, 2021, DOI: 10.1016/j.arabjc.2021.103500
48. **Aboulthana W, Ibrahim N, Osman NM, Seif M, Hassan A, Youssef AM, El-Feky AM, Madboli A:** Evaluation of the biological efficiency of silver nanoparticles biosynthesized using *Croton tiglium* L. seeds extract against azoxymethane induced colon cancer in rats. *Asian Pac J Cancer Prev,* 21, 1369-1389, 2020. DOI: 10.31557/apjcp.2020.21.5.1369